

## Article

# Structural Characterization, Antioxidant, and Antiviral Activity of Sulfated Polysaccharide (Fucoidan) from *Sargassum asperifolium* (Turner) J. Agardh

Abeer A. Ageeli \*  and Sahera Fathalla Mohamed 

Chemistry Department, College of Science, Jazan University, P.O. Box. 114, Jazan 45142, Saudi Arabia

\* Correspondence: abeerali@jazanu.edu.sa

**Abstract:** Brown algae possess a diverse array of acidic polysaccharides, including fucoidan. The present research intends to investigate the extraction and characterization of algal polysaccharides to explore their antiviral activity. A light brown sulfated polysaccharide was extracted (with a yield of 18% of dry weight) from *Sargassum asperifolium* algal powder. The results of fractionation of sulfated polysaccharide revealed the occurrence of two primary fractions: low-sulfated polysaccharides (SPF1) and high-sulfated polysaccharides (SPF2). The bioassays conducted on SPF2 demonstrated a greater level of antioxidant activity compared to SPF1, with respective  $IC_{50}$  values of  $17 \pm 1.3 \mu\text{g/mL}$  and  $31 \pm 1.1 \mu\text{g/mL}$  after a duration of 120 min. The cytotoxicity of SPF2 on Vero cells was determined, and the calculated half-maximal cytotoxic concentration ( $CC_{50}$ ) was found to be  $178 \pm 1.05 \mu\text{g/mL}$ . Based on these results, an antiviral activity assay was conducted on SPF2. The results demonstrated that SPF2 had greater efficacy against Hepatitis A Virus (HAV) compared to Herpes Simplex Virus Type 1 (HSV-1), with corresponding half-maximal inhibitory concentrations ( $IC_{50}$ ) of  $48 \pm 1.8 \mu\text{g/mL}$  and  $123 \pm 2.6 \mu\text{g/mL}$ , respectively. The active SPF2 was characterized by FT-IR,  $^1\text{H}$ , and  $^{13}\text{C}$  NMR spectroscopy. The extracted fucoidan can be used as a natural therapeutic agent in combating various viral infections.

**Keywords:** brown algae; fucoidan; *Sargassum asperifolium*; antioxidant; antiviral activity



**Citation:** Ageeli, A.A.; Mohamed, S.F. Structural Characterization, Antioxidant, and Antiviral Activity of Sulfated Polysaccharide (Fucoidan) from *Sargassum asperifolium* (Turner) J. Agardh. *Chemistry* **2023**, *5*, 2756–2771. <https://doi.org/10.3390/chemistry5040176>

Academic Editors: Massimiliano Fenice and M. Amparo F. Faustino

Received: 14 November 2023

Revised: 5 December 2023

Accepted: 9 December 2023

Published: 12 December 2023



**Copyright:** © 2023 by the authors. Licensee MDPI, Basel, Switzerland. This article is an open access article distributed under the terms and conditions of the Creative Commons Attribution (CC BY) license (<https://creativecommons.org/licenses/by/4.0/>).

## 1. Introduction

In recent years, there has been a notable surge in the prevalence of viral diseases, resulting in significant detrimental effects on human health [1]. Diverse natural products, primarily derived from marine macroalgae (seaweeds), are regarded as viable alternative treatments for multiple viral diseases [2–4]. Marine seaweeds consist of a complex of dynamic cell walls rich in different types of polysaccharides, such as alginate, laminaran cellulose, and fucoidan [5]. Due to the vast variation in their molecular weight and structural parameters, seaweed sulfated polysaccharides are already well-known for their anti-inflammatory, antiproliferative, anticoagulant, and antioxidant properties and inhibit adipogenesis [6–8]. Algal sulfated polysaccharides gained attention as an antiviral agent due to their multiple biological activities and safety [9–11].

Sulfated polysaccharides (SP) represent the prevailing anionic polymers among the macroalgal community. Cellular damage and subsequent cell death are caused by reactive oxygen species (ROS) and the destruction of cellular macromolecules, including membrane lipid peroxidation. Therefore, scientists have pursued targeting marine sulfated polysaccharides for natural antioxidants. Reportedly, these sulfated polysaccharides delay or prevent oxidation by either scavenging ROS or inhibiting the production of ROS [12]. Fucoidan is a unique sulfated polysaccharide found in the cell wall matrix of brown algae. The predominant component of fucoidan is fucose, but it also contains other monomers, such as xylose, galactose, mannose, and glucuronic acid [13]. The antiviral mechanism of sulfated polysaccharides is specific to their structure and virus type. For instance, coronaviruses

are enveloped, positive-stranded RNA viruses with cytoplasmic replication [14]. In order to deliver the nucleocapsid into the host cell, the coronavirus-cell entry procedure entails the fusion of the envelope with the host cell membrane, which is primarily determined by viral S proteins [14,15]. Negatively charged sulfated polysaccharides can interact with the surface of a virus, preventing it from replicating or killing it directly. The antiviral mechanism of fucoidans may involve preventing the attachment of the herpes simplex virus (HSV)-2 virion to host cells [16].

Herpes simplex viruses (HSV-1) are a form of linear double-strand DNA virus composed of at least 18 proteins and a complex spherical structure with four layers. It is a member of the  $\alpha$ -herpesvirus subfamily [17]. The rate of adult herpes simplex virus-1 infection ranges from 60% to 95% [18]. It can induce diseases, such as herpes simplex keratitis, conjunctivitis, and labialis, among others. Recurrent HSV-1-caused eye infections are one of the leading causes of blindness [19]. In addition, it has been reported that HSV-1 is an Alzheimer's disease (AD) risk factor [20]. Hepatitis A virus (HAV) is a picornavirus; it lacks an envelope and comprises a single strand of positive-sense RNA encased in a protein shell [21].

Our previous studies on sulfated polysaccharides from *S. latifolium* and *Padina pavonia* demonstrated significant antiviral activity against the HSV-1 and HAV viruses [22,23]. Sulfated polysaccharides from *Sargassum wightii* have been shown to be hepatoprotective [24].

*Sargassum* (family Sargassaceae, of the order Fucales, subclass Cyclosporeae, and class Pheophyceae) is a genus of brown algae, commonly known as gulfwed. *Sargassum* was discovered by Agardh in 1820 and is reported to contain 537 species distributed worldwide [25]. *Sargassum asperifolium* was found to be the predominant species growing along the Farasan Island shores. The objective of the current study is to assess the antioxidative and antiviral properties of sulfated polysaccharide derived from *Sargassum asperifolium*, a new species from a unique collection site, to assess its potential to be a new candidate for this purpose.

## 2. Materials and Methodology

### 2.1. Algal Material

*Sargassum asperifolium* (Turner) J. Agardh was selected for this study.

### 2.2. Collection Site

The brown algal sample was collected from Farasan Island, as depicted in Figure 1, located approximately 50 km off the coastline of Jazan city in the extreme southwest of Saudi Arabia. Farasan Island is one of the largest islands in the Red Sea (16°48'0" N, 41°51'0" E). The collection took place between April and May of 2022. The sample underwent a thorough cleaning process, where it was washed with seawater to remove rocks and epiphytes, brushed with flowing tap water, and subsequently air-dried at room temperature. Following the drying process, the sample was finely ground into powder and then stored in a dry, cold location until its use.

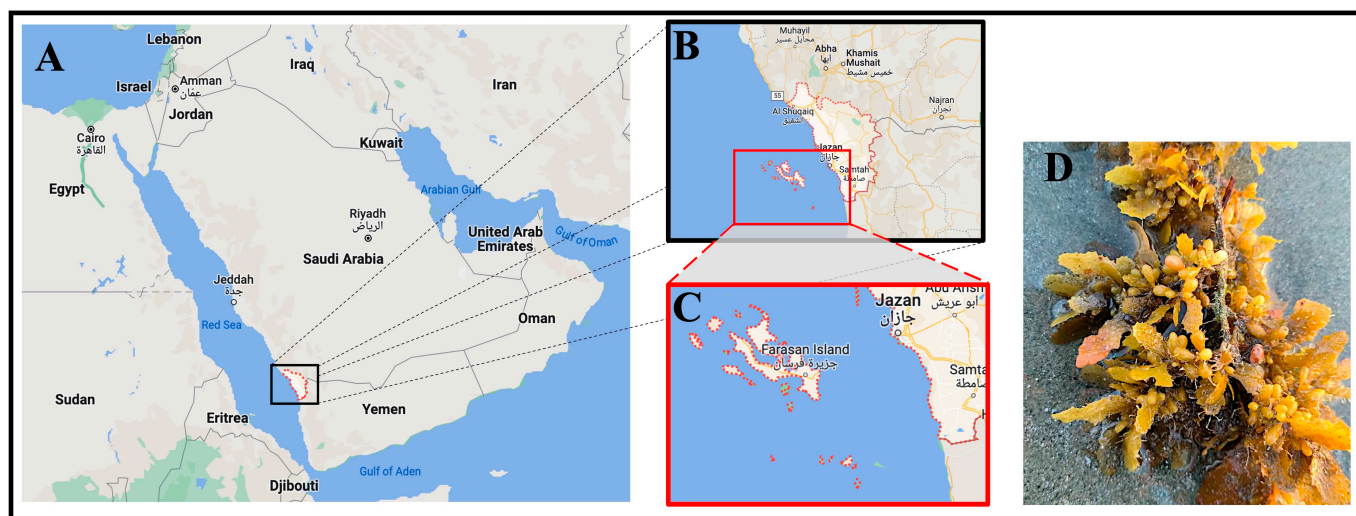


**Figure 1.** (A) The map of the Arabic peninsula shows the location of Jazan city in black box, located in the southwest region of Saudi Arabia. (B,C) Zoomed-in illustrations of Jazan city and Farasan Island, where the algae samples have been taken. It can be seen that Farasan Island is close to Jazan city, approximately 50 km away. Panels (A–C) were obtained from Google Maps [26]. (D) The brown algae that has been collected for the study.

### 2.3. Extraction

The total sulfated polysaccharide SP was extracted using the previously reported method with some modifications [27,28]. A sample of 10 g of algal powder was steeped overnight at room temperature in 100 mL of a mixture solution of MeOH/CHCl<sub>3</sub>/H<sub>2</sub>O (4:2:1) to remove lipids, pigments, and other low molecular weight compounds. The suspension was then filtered, and the residue was rinsed multiple times with the same mixture until a clear-colored filtrate emerged, suggesting that defatting was complete. The recovered algal biomass was then desiccated at 50 °C for 24 h before being suspended in distilled water (1:20) at 80 °C for 6 h in a shaker water bath. After 15 min of centrifugation at 3000 rpm, the supernatant was removed. The algal residue was extracted three times with boiling water, and the supernatants were collected and precipitated overnight at 4 °C using 3 volumes of absolute ethanol. The precipitate was centrifuged at a rate of 10,000 × *g* for 20 min. The white fibrous desiccated polysaccharide was suspended in water and dialyzed against distilled water for 48 h, after which it was lyophilized and stored in a cool, dry area until use.

### 2.4. Fractionation and Purification of Polysaccharide

We dissolved 180 mg of lyophilized SP extract in distilled water and fractionated it using a DEAE-Sephadex column (50 cm × 2.5 cm i.d.). Then, it was eluted with a step gradient from 0 to 1.0 M NaCl at a flow rate of 1 mL/min. Five-milliliter fractions were collected each time. The carbohydrate-high-sulfated fractions were identified [29]. There were two regular peaks on the elution profile, which were grouped into two main fractions. The two fractions were dialyzed against deionized water before being lyophilized. Each fraction was subjected to purification by gel filtration chromatography using Sephacryl S-300 (80 cm × 2.5 cm, i.d.) column. Each fraction was dissolved in 1 mL of 0.1 M NaCl and then applied to the column. Elution was carried out by using 0.1 M NaCl at a flow rate of 0.5 mL/min. The purified fractions were categorized as low-sulfated fraction (SPF1) and high-sulfated fraction (SPF2), which were then dialyzed and lyophilized for further experiments.

### 2.5. Monosaccharide Analysis

The monosaccharide composition of both SPF1 and SPF2 was analyzed using high-performance liquid chromatography (HPLC). Both fraction samples (30 mg) were hydrolyzed for 5 h at 105 °C using 5 mL of 88% formic acid in a sealed tube [30]. Excess formic acid was removed using multiple washes with deionized water to ensure the elimination of any remaining formic acid. Then, the samples were dissolved in absolute ethanol to collect only monosaccharides. After that, the ethanol was evaporated using SpeedVac. Finally, the precipitate was dissolved in deionized water before analysis. Using Agilent HPLC model 1100 series (Agilent Technologies, Santa Clara, CA, USA), the monosaccharide concentration was determined [31]. Following the Official Methods of Analysis (AOAC, 1996), the uronic acid content of the test sample was determined. The blank in this experiment was 2 mol/L sulfuric acid. As a standard, a 6.25–400 µg/mL solution of D-galacturonic acid was utilized. Each sample's uronic acid concentration was expressed as a percentage by weight (% *w/w*).

### 2.6. Determination of Total Sulfate Content

The sulfate content of polysaccharides was determined in both SPF1 and SPF2. Magnesium sulfate was used as a standard [32].

### 2.7. Determination of Relative Molecular Weight of Both SPF1 and SPF2

HPLC (Hewlett-Packard series 1100 HPLC system, Agilent GPC-Addon, Waldbronn, Germany) was used to determine the average molecular mass of purified polysaccharides SPF1 and SPF2. The sample (1.00 g/L) of each was dissolved in 0.5 mol/L NaCl before being eluted with water. The eluted component was detected using a Refractive Index detector (HP 1047A RI Detector, Santa Clara, CA, USA). As molecular markers, Dextran standards (Fluka) of MW 25, 80, 270, and 670 kDa were utilized to determine the average molecular weight of the sample [33–35].

### 2.8. Fourier Transform Infrared (FT-IR) Spectroscopy

The powdered extracts, SPF1 and SPF2, approximately 1 mg of each, were sampled and mixed well with dry potassium bromide of infrared grade (IR grade). The samples were pressed into a disc to create a film, and then placed in the holder of the spectroscope (Shimadzu PC 8201, Kyoto, Japan). The spectra were recorded within 400–4000 cm<sup>-1</sup> wavelength region [34,36].

### 2.9. <sup>1</sup>H and <sup>13</sup>C Nuclear Magnetic Resonance (<sup>1</sup>H and <sup>13</sup>C NMR) Spectroscopy

This analysis was conducted on powdered SPF2, polysaccharide. A Varian INOVA 600 MHz spectrometer was used to record <sup>1</sup>H and <sup>13</sup>C spectra of the sample in D<sub>2</sub>O as solvent (4 mg in 0.55 mL) at 25 °C.

### 2.10. DPPH Free Radical Scavenging Activity

The free radical scavenging properties of polysaccharides SPF1 and SPF2 were assessed as reported in previous work with some modifications [37]. A fresh solution of 1,1-diphenyl-2-picryl-hydrazyl (DPPH) was prepared in 100 mL of absolute methanol at a concentration of 0.1 mM, and 1 mL of this solution was added to 1 mL of each polysaccharide sample and ascorbic acid (reference drug) at various concentrations (10–50 µg/mL). The mixture was vigorously agitated and allowed to rest in the dark for 30, 60, 90, and 120 min before measurement. The absorbance was measured at 517 nm against a blank using a UV/VIS 2401PC spectrophotometer (Shimadzu, Kyoto, Japan). At a minimum, measurements were obtained in triplicate. The capacity to scavenge was determined using the following equation:

$$\text{DPPH Scavenging ability (\%)} = (A_c - A_t) / A_c \times 100$$

where  $A_c$  is the absorbance of DPPH solution without a sample (control),  $A_t$  is the absorbance of DPPH solution with the tested polysaccharide sample.

The  $EC_{50}$  value is the effective concentration ( $\mu\text{g}/\text{mL}$ ) of SPF1 and SPF2 at which the DPPH radicals were scavenged by 50%.

### 2.11. Antiviral Activity of SPF2

#### 2.11.1. Mammalian Cell Line

The Vero cell lines (derived from the kidney of a normal African green monkey) were granted by the American Type Culture Collection (ATCC, Manassas, VA, USA). DMEM supplemented with 10% heat-inactivated fetal bovine serum (FBS), 1% L-glutamine, HEPES buffer, and 50  $\mu\text{g}/\text{mL}$  gentamycin was used to grow the Vero Cell. All cells were subcultured twice per week at 37 °C in a humidified atmosphere containing 5%  $\text{CO}_2$  [38].

#### 2.11.2. Virus Propagation

On confluent Vero cells, the cytopathogenic HSV-1 and HAV viruses were propagated and tested [39]. Using the Spearman–Karr method, viruses were counted to determine the 50% tissue culture infectious dose ( $TCID_{50}$ ) with eight wells per dilution and 20  $\mu\text{L}$  of inoculum per well [40].

#### 2.11.3. Cytotoxicity Evaluation Using Viability Assay

In the cytotoxicity assay, the Vero cell line was inoculated in 96-well plates at a concentration of  $2 \times 10^5$  cells/mL in 100  $\mu\text{L}$  of growth medium [41]. After 24 h of inoculation, fresh medium was added, including different concentrations of the tested sample. Using a multichannel pipette, 2-fold dilutions of SPF2 polysaccharide (beginning at 2–1000  $\mu\text{g}/\text{mL}$ ) were added to confluent cell monolayers dispensed into 96-well, flat-bottomed microtiter plates (Falcon, Jersey, NJ, USA). The microtiter plates were incubated for 48 h at 37 °C in a humidified incubator with 5%  $\text{CO}_2$ . Three wells were utilized for each examined sample concentration. Control cells were incubated with or without DMSO and a polysaccharide sample. The minuscule amount of DMSO found in the wells (no more than 0.1%) did not affect the experiment. At the end of the incubation period, the mitochondrial-dependent reduction of yellow MTT (3-(4,5-dimethylthiazol-2-yl)-2,5-diphenyl tetrazolium bromide) to purple formazan was used to determine cell viability [42,43]. The media was removed from the wells and replaced with 100  $\mu\text{L}$  of fresh culture medium, followed by the addition of 10  $\mu\text{L}$  of the yellow MTT [12 mM MTT stock solution (5 mg/mL PBS)] to each well, including the untreated controls. The 96-well plates were then incubated for 4 h at 37 °C and 5%  $\text{CO}_2$ . An Aliquot of the media (85  $\mu\text{L}$ ) was removed from the wells, and 50  $\mu\text{L}$  of DMSO was added to each well. The plate was correctly shaken for 5 min to mix the formazan produced by viable cells with the solvent and then incubated at 37 °C for 10 min. Using the microplate reader (SunRise, TECAN, Inc., Morrisville, NC, USA), each well's optical density (OD) was measured at 590 nm and subtracted from the background at 620 nm. Each experiment was conducted in triplicate, and the percentage of relative cellular viability was calculated relative to untreated control cells.

$$\% \text{ Cell viability} = [(OD_t/OD_c)] \times 100$$

where  $OD_t$  and  $OD_c$  correspond to the average optical density of wells treated with the test sample and the average optical density of untreated cells, respectively. The relationship between surviving cells and the evaluated polysaccharide SPF2 concentration is graphed to obtain the Vero cell line survival curve following treatment. The cytotoxicity concentration ( $CC_{50}$ ) is the polysaccharide concentration that exerts half of the maximum inhibitory effect and inhibits 50% of cell growth. Using GraphPad Prism software (San Diego, CA, USA), the  $CC_{50}$  was estimated from graphic depictions of the dose-response curve for each concentration. The maximal nontoxic concentration (MNTC) of SPF2 was determined and used in subsequent antiviral studies. Regarding the cytotoxicity assay and data analysis,

all experiments and data analysis were conducted at the Regional Center for Mycology and Biotechnology (Al-Azhar University, Cairo, Egypt).

#### 2.11.4. Antiviral Assay

The screening antiviral assay system was established at the Regional Center for Mycology and Biotechnology (RCMB) at Al-Azhar University, Egypt, using a cytopathic effect inhibition assay. The assay was chosen to demonstrate specific inhibition of a biological function, namely cytopathic effect (CPE), in sensitive mammalian cells as measured by the MTT technique [44,45]. Monolayers of Vero cells ( $2 \times 10^5$  cells/mL) adhered to the bottom of the wells in a 96-well microtiter plate and were incubated for 24 h at 37 °C in a humidified incubator containing 5% CO<sub>2</sub>. The cultures were subjected to a simultaneous treatment involving two-fold serial dilutions of SPF2 in a newly prepared maintenance medium. Following this, the cultures were incubated at a temperature of 37 °C for 48 h. Prior to the incubation, the plates were rinsed with fresh DMEM and subsequently exposed to 10<sup>4</sup> doses of HSV-1 and HAV viruses. In order to investigate the impact of SPF2 (specific factor) on infection control, two experimental groups were established: one group without SPF2 (referred to as the absence of the SPF2 group) and another group without any infection controls or treatment of Vero cells (referred to as the untreated Vero cell control group). A total of six wells were employed to measure the concentration of SPF2 in the experiment. The assessment of the antiviral activity involved the comparison of cytopathic effect inhibition with a control group, specifically examining the protective effects of SPF2 on the cells. Three separate experiments were evaluated. The cyclovir drug served as the positive control in this assay. Following the incubation period, cell viability was determined using the MTT assay, as described previously in the cytotoxicity section.

The viral inhibition rate was calculated as follows:  $[(A - B)/(C - B)] \times 100\%$

The variables A, B, and C represent the absorbance values of the tested compound (SPF2) in the presence of virus-infected cells, the absorbance of the viral control, and the absorbance of the cell control, respectively.

Based on the graphical plots, the IC<sub>50</sub> (50% inhibition dose) of the viral infection has been determined using the available data in relation to the virus control. The IC<sub>50</sub> values were directly calculated by graphing the inhibition of viral yield against the concentration of the samples. The selectivity index (SI) was calculated by comparing the CC<sub>50</sub> to IC<sub>50</sub> ratios [46]. This calculation aimed to evaluate if the SPF2 polysaccharide possessed antiviral properties that were superior to its level of toxicity. It was reported before that any compound with a structural integrity (SI) value equal to or greater than 2 was deemed to possess activity [38].

#### 2.12. Statistical Analysis

Statistical analysis of antioxidants is carried out using two-way ANOVA coupled with a CO-state computer program. Data on cytotoxicity and antiviral activity were analyzed by one-way analysis of variance (ANOVA) using the Statistical Package for the Social Sciences (SPSS) program, version 14 (IBM Software, Armonk, NY, USA). The difference was considered significant at  $p < 0.05$ .

### 3. Results and Discussion

#### 3.1. Extraction and Purification of the Sulfated Polysaccharide via Chromatography

On a dry weight basis, the extraction yield of crude sulfated polysaccharide from the desiccated algal sample *S. asperifolium* was approximately 18%. A schematic illustration of the purification procedure is depicted in Figure 2A. The crude extract was fractionated on a DEAE Sephadex column using a step gradient from 0 to 1.0 M NaCl. Two main fractions, designated SPF1 and SPF2 (Figure 2B), were obtained. The ability of SPF2 to bind to DEAE-cellulose and then be eluted with NaCl solution suggests that SPF2 is anionic in nature. The fraction SPF1, however, did not attach to the anion exchanger and was quickly washed away with water containing a very low concentration of NaCl. It was a polysaccharide

with a minor anion charge. According to the results of the sulfate determination test, both fractions contained sulfate, but SPF2 contained 15.32% and SPF1 contained 9.65% (Table 1). The average sulfate content of *S. asperifolium* falls within the 9–40% range reported for the genus *Sargassum* [47–50]. Additional esterification of the R-O-SO<sub>3</sub>-groups of the polysaccharide could account for the neutral nature of SPF1 sulfated polysaccharide [51].

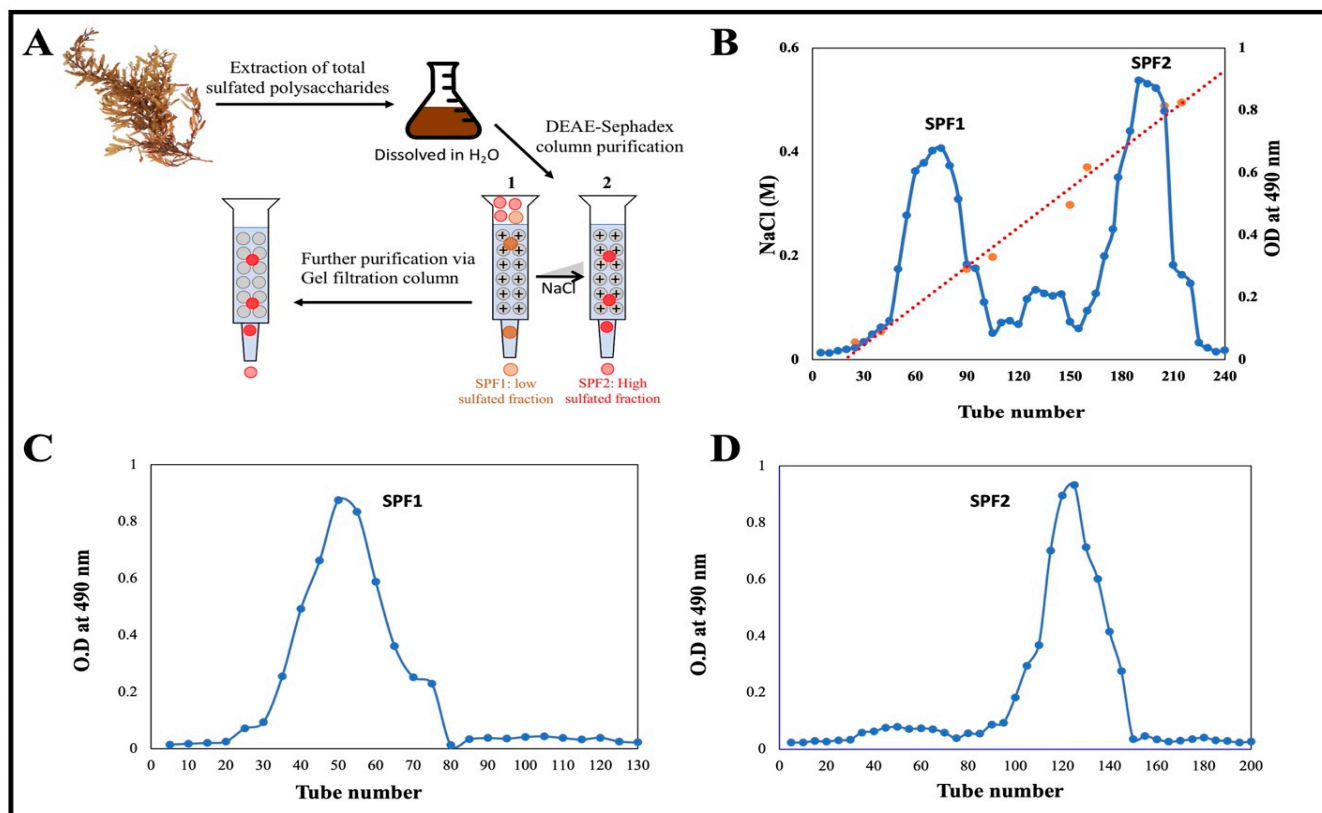


**Figure 2.** (A) An illustration of the purification processes of sulfated polysaccharides using various chromatography techniques. Different color dots represent a mixture of different molecules and the variation in their movement along the column. (B) Ion exchange chromatography of sulfated polysaccharide on the DEAE Sephdex column. The crude extract was dissolved in distilled water and applied on column. The column was eluted with 0–1.0 M NaCl. The carbohydrates in each fraction were determined by phenol-H<sub>2</sub>SO<sub>4</sub>. (C,D) Gel filtration chromatography of SPF1 and SPF2 on Sephacryl S-300 column, respectively. The column was eluted with 0.1 M NaCl. Each fraction was determined by phenol-H<sub>2</sub>SO<sub>4</sub>.

**Table 1.** Chemical composition, sulfate contents, weight-average (Mw), number-average (Mn), and polydispersity (PI) of the sulfated polysaccharides SPF1 and SPF2.

SP	Molecular Mass Moments (g/mol or Da)			Monosugars Molar Ratio				Uronic Acid %	Sulfate %
	Mw	Mn	PI *	Glucuronic Acid	Glucose	Mannose	Fucose		
SPF1	$5.49 \times 10^5$	$4.95 \times 10^5$	1.1	1.8	2.8	1.9	1.0	21.08	9.65
SPF2	$3.46 \times 10^5$	$1.97 \times 10^5$	1.75	1.6	2.5	1.0	1.8	25.34	15.32

SPF1: low-sulfated polysaccharide fraction mainly eluted with 0.4 M NaCl in anion exchange chromatography.  
 SPF2: high-sulfated polysaccharide fraction mainly eluted with 0.55 M NaCl in anion exchange chromatography.  
 \* PI: polydispersity = Mw/Mn of the polysaccharide.

Further purification of SPF1 and SPF2 was performed by gel filtration chromatography on a Sephacryl S-300 column using a 0.1 M NaCl solution for elution (Figure 2C,D). It was discovered that SPF1 and SPF2 each had a single peak. By comparing SPF1 and SPF2 to a standard dextran molecular marker, the relative molecular weight of both was calculated. They were two molecule-sized compounds. Table 1 shows that the average Mw of SPF1 and SPF2 was  $5.49 \times 10^5$  Da and  $3.46 \times 10^5$  Da, respectively. These values lie within the ranges previously reported for fucoidan obtained (18–359 kDa) [52]. Other fucoidan Mw values have been reported for *Ascophyllum nodosum*, *Saccharina longicuris*, and *Fucus vesiculosus* (417, 454, and 529 kDa, respectively), which are too close to the value found for *S. asperifolium* [49]. The variation in fucoidans Mw has been linked to species-specific, seasonal variations and the processing conditions used to extract the biomolecules [52].

### 3.2. Monosaccharide Compositions of Purified Polysaccharides SPF1 and SPF2

The polysaccharide composition of the purified polysaccharides is shown in Table 1. SPF1 was characterized by a higher content of glucose and mannose than SPF2. The fucose concentration in SPF2 was roughly twice that of SPF1. The monosaccharide composition indicates that SPF1 is predominantly laminaran due to its high glucose and mannose content, whereas SPF2 is predominantly fucoidan because of its high fucose content. Previous studies have demonstrated that brown seaweed fucoidan contains significant amounts of fucose [13,53,54].

### 3.3. FT-IR Analysis

The FT-IR spectra of both SPF1 and SPF2 are presented in Figure 3 and Table 2. The major absorption bands between 3405 and 3445  $\text{cm}^{-1}$  and bands between 2924 and 2961  $\text{cm}^{-1}$  are attributed to the O-H stretching of hydroxyls and the CH stretching peak of  $\text{CH}_2$  groups, respectively. The absorption bands located between 1410 and 1456  $\text{cm}^{-1}$  are attributed to the symmetric stretch vibration of  $\text{COO}^-$  and the stretch vibration of C-O within  $\text{COOH}$  [55]. In addition, the absorption bands between 1229 and 1251  $\text{cm}^{-1}$  and 1307 and 1321  $\text{cm}^{-1}$  have been identified as S=O stretching vibrations, indicating the presence of esterified sulfate. The band between 825 and 840  $\text{cm}^{-1}$  is attributed to the bending vibration of sulfate's C-O-S. The peaks at 1148.4 and 1032.6  $\text{cm}^{-1}$  in the polysaccharide fingerprint region of 1200–800  $\text{cm}^{-1}$  were attributed to vibrations of C-O-C glycosidic bonds [56]. The  $\beta$ -pyranose peaks at 941.0 and 892.8  $\text{cm}^{-1}$  have been identified [57]. The modest absorption at 820.5  $\text{cm}^{-1}$  may be attributable to the presence of mannose, which is consistent with the compositional results of monosaccharides [58]. The FTIR results were completely consistent with previously published results concerning the structural analysis of fucoidan [59].

**Table 2.** FT-IR spectra of purified sulfated polysaccharide of *S. asperifolium* in the frequency range 400–4000  $\text{cm}^{-1}$ .

Sample	Frequency ( $\text{cm}^{-1}$ ) of Spectra						
	1229–1252	825–840	3405–3445	2924.08	2121–2143	1410–1456	1035–1070
SPF1	1219.76	819.59	3373.85	2926.45	2113.6	1431.89	1030.77
SPF2	1237.11	820.563	3433.64	2919.7	2116.49	1425.14	1032.69
Functional group	S=O	C-O-S	O-H	C-H	Fucose	CO within COOH	C-O-C glucosides

SPF1: low-sulfated polysaccharide fraction mainly eluted with 0.4 M NaCl in anion exchange chromatography, SPF2: high-sulfated polysaccharide fraction mainly eluted with 0.55 M NaCl in anion exchange chromatography.

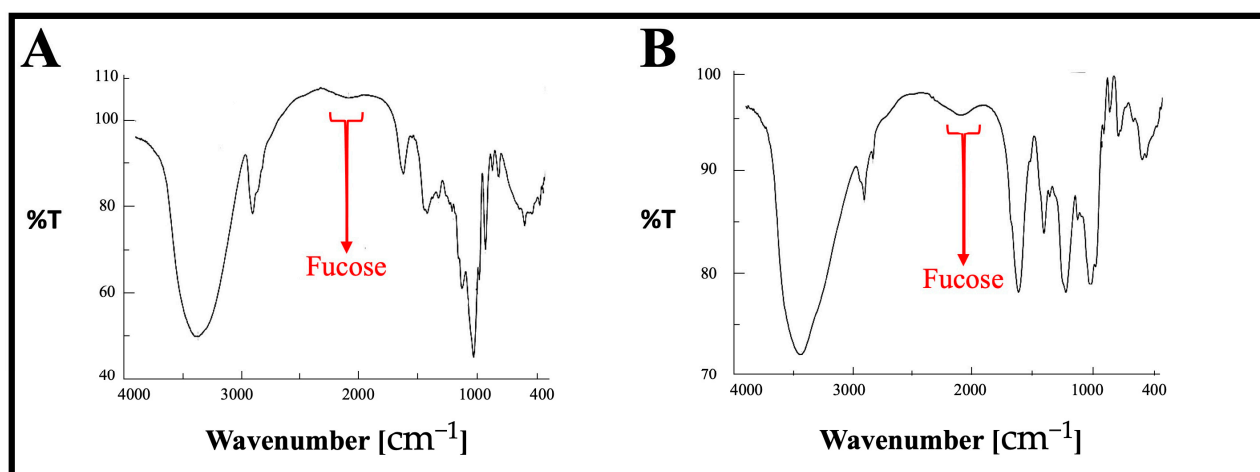


**Figure 3.** FT-IR spectrum of the purified polysaccharides, SPF1 (A) and SPF2 (B), extracted from *S. asperifolium*. The red arrows represent the fucose peak in both samples.

### 3.4. $^1\text{H}$ and $^{13}\text{C}$ NMR Spectroscopy

The  $^1\text{H}$  and  $^{13}\text{C}$  NMR spectra of polysaccharide (SPF2) are presented in Figure 4A,B. The presence of polysaccharide was confirmed by the presence of anomeric proton signals in the downfield region ( $\delta$  3.0–5.5 ppm) of the  $^1\text{H}$  NMR spectrum (Figure 4A). The signal at  $\delta$  5.15 ppm was identified as the proton anomer in glucose [60]. The integral ratios observed within the two regions, specifically  $\delta$  4.8–5.6 ppm and  $\delta$  3.3–4.2 ppm, suggest the presence of several monosaccharide structures. This finding supports the notion that the substance under investigation (referred to as SPF2) is a heteropolysaccharide. These results align with the outcomes obtained from both the monosaccharide analysis and the FT-IR study. The  $\alpha$ -type configuration appears in the  $^1\text{H}$  NMR spectrum at 4.8–5.6 ppm, and the  $\beta$ -type configuration appears at  $\delta$  4.4–4.8 ppm [61]. Consequently, the signals at  $\delta$  4.58,  $\delta$  4.66, and  $\delta$  4.68 ppm correspond to  $\beta$ -glycosidic bonds [62]. Signal at  $\delta$  4.81 ppm indicated the presence of hydrogen-containing sulfate at C4 position. The H2-H6 signatures in SPF2 had peaks between  $\delta$  4.07 and  $\delta$  3.48 ppm. The  $^{13}\text{C}$  NMR spectrum of SPF2 (Figure 4B) revealed an anomeric carbon signal at  $\delta$  103.25 ppm. C4 with a sulfate moiety was detected as a peak at  $\delta$  81.25 ppm, while the position of C3 was confirmed by a signal at  $\delta$  76.57 ppm [63–65]. Peaks at  $\delta$  61.53–81.60 ppm, signal of C2–C6 resonance in residual hexose, but  $\delta$  103.25 ppm attributed to C1 of fucose, are consistent with HPLC results. The absence of  $\delta$  82–88 ppm signals in  $^{13}\text{C}$  NMR spectra indicated that all residual sugars were in the pyranose form [55]. Fucoidan is a sulfated polysaccharide typically derived from brown algae, and the results of the FT-IR and NMR analyses of the SPF2 fraction were in perfect agreement with the reports on fucoidan.

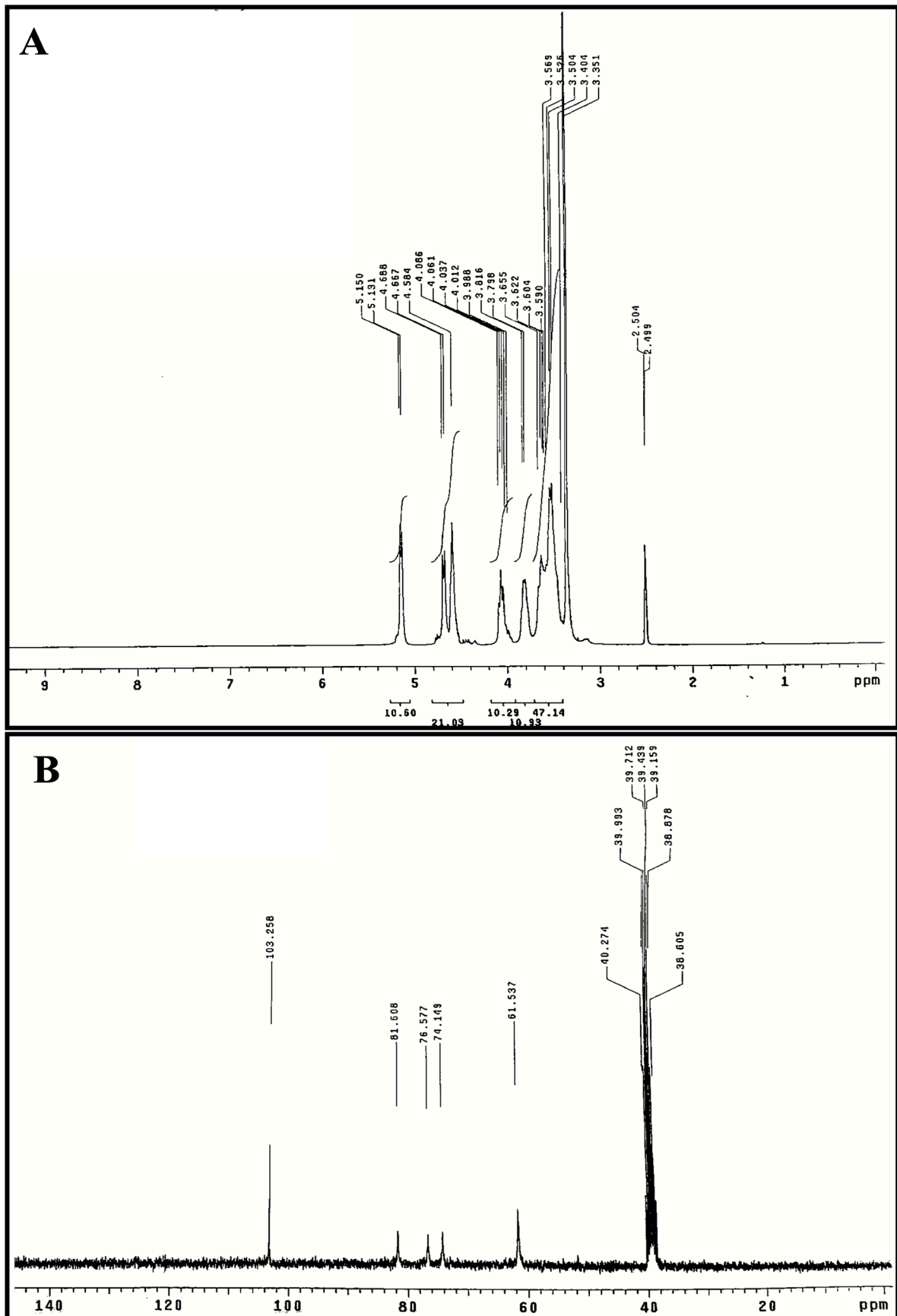
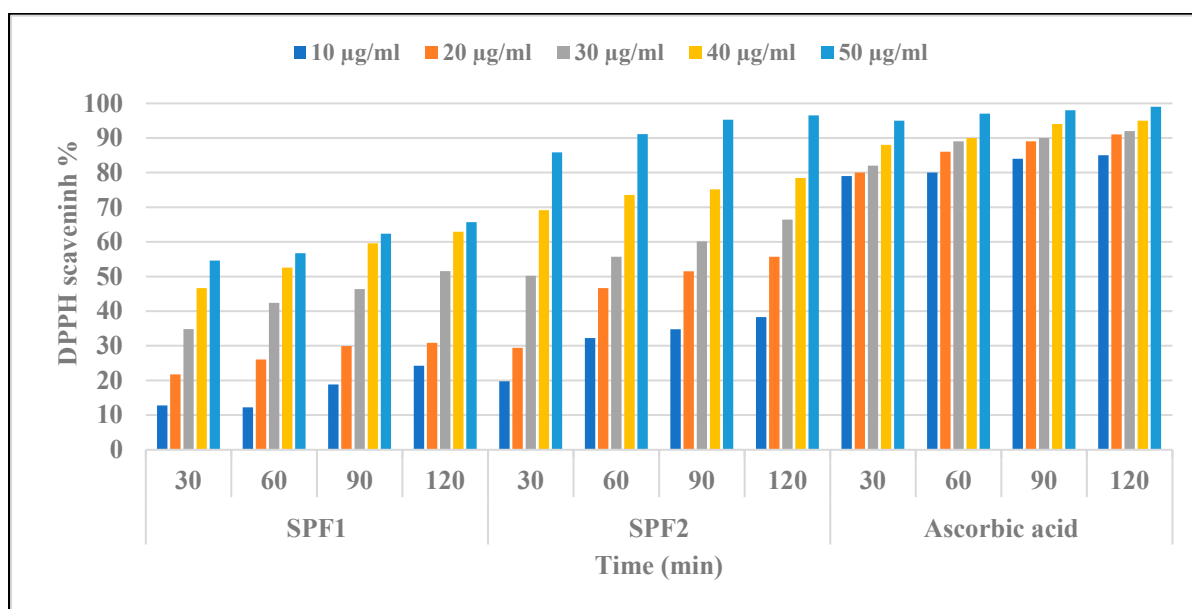


Figure 4. NMR spectra of the purified polysaccharide SPF2 extracted from *S. asperifolium*,  $^1\text{H}$  NMR spectrum (A) and  $^{13}\text{C}$  NMR spectrum (B).

### 3.5. Assessment of In Vitro Antioxidant Activity of SPF1 and SPF2 Polysaccharides

The antioxidant activities of algal polysaccharides are closely related to their physicochemical properties, such as sulfate group content, uronic acid content, and molecular weight [66]. Compounds with the functional groups -OH, -SH, C=O, COOH, -S, and S-O-S have been shown to be more effective at scavenging free radicals [67]. Figure 5 demonstrates a linear increase in free radical quenching activity for both SPF1 and SPF2 fractions compared with ascorbic acid as a control, but the scavenging activity of DPPH by SPF2 was greater than that of SPF1. It was also observed that scavenging activity depended on the period of treatment as well as the concentration of each polysaccharide. SPF2 displayed the greatest inhibition effect with IC<sub>50</sub> values of 30 ± 2.1, 24 ± 0.3, 19 ± 0.82, and 17 ± 1.3 µg/mL after 30, 60, 90, and 120-min ration, whereas SPF1 displayed IC<sub>50</sub> values of 45 ± 1.5, 37 ± 0.81, 33 ± 1.2, and 31 ± 1.1 µg/mL after 30, 60, 90, and 120-min ration. The results also showed a negative correlation between antioxidant activity and sulfated polysaccharide fractions, SPF1 and SPF2, that may be related to the non-compact structure of low-MW SPF2 and, consequently, the more potentially available hydroxyl groups reacting with free radicals [68].



**Figure 5.** In vitro antioxidant activity of sulfated polysaccharides SPF1 and SPF2 extracted from *S. aserifolium* and ascorbic acid by measuring the DPPH scavenging effect (%) at various concentrations and different times. SPF1: low-sulfated polysaccharide fraction mainly eluted with 0.4 M NaCl in anion exchange chromatography. SPF2: high-sulfated polysaccharide fraction mainly eluted with 0.55 M NaCl in anion exchange chromatography.

### 3.6. In Vitro Cytotoxicity of SPF2 Polysaccharide

Before studying the antiviral effect of sulfated polysaccharide extracted from *S. aserifolium*, SPF2, which was used in this study, it was imperative to determine its maximum nontoxic level. MTT ((3-(4,5-dimethylthiazol-2-yl)-2,5-diphenyl tetrazolium bromide) assay was performed to determine the cytotoxic properties of Vero cell lines. As shown in Figure 6A, the number of viable Vero cells decreases as the concentration of polysaccharides increases. A concentration of 50 µg/mL kept the viability of Vero cells to approximately 90%, while the concentration that was cytotoxic to 50% of Vero cells (CC<sub>50</sub>) was determined to be 178 ± 1.05 µg/mL.

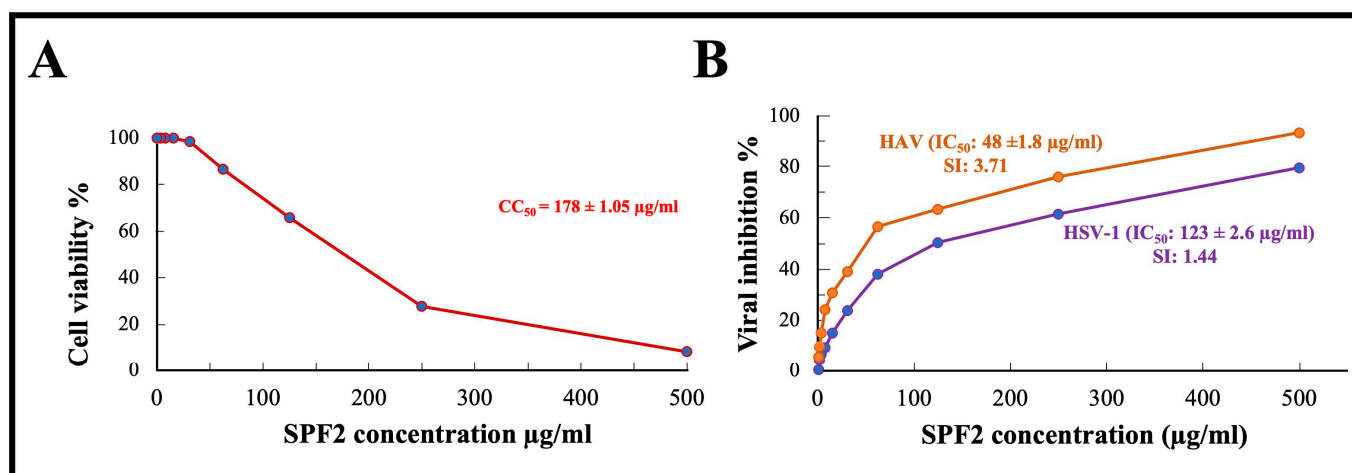


**Figure 6.** (A) In vitro cytotoxic effect of the isolated sulfated polysaccharide SPF2 against Vero cells. (B) Antiviral activity of sulfated polysaccharide fraction SPF2 against both HSV-1 and HAV in Vero cells. SPF2: high-sulfated polysaccharide fraction mainly eluted with 0.55 M NaCl in anion exchange chromatography.  $CC_{50}$ : concentration of sulfated polysaccharide is cytotoxic to 50% of Vero cells,  $IC_{50}$ : concentration of sulfated polysaccharide that inhibits viral infectivity (cytopathic effect) by 50%, SI: selective index =  $CC_{50}/IC_{50}$ .

### 3.7. Antiviral Activity of SPF2 Polysaccharide

The antiviral activity of the isolated sulfated polysaccharide SPF2 isolated from *S. asperifolium*, was assayed by using MTT, the assay chosen to demonstrate specific inhibition of a biological function, cytopathic effect (CPE), in sensitive mammalian cells. Cytopathogenic HSV-1 and HAV viruses were propagated and tested in confluent Vero cells. MTT is reduced in metabolically active cells to yield an insoluble purple formazon product. Our results demonstrate that SPF2 had a potent inhibitory effect on the HAV virus, with an  $IC_{50}$  of  $48 \pm 1.8 \mu\text{g/mL}$  and a selective index (SI) of 3.71, whereas its effect on HSV-1 was less potent, with an  $IC_{50}$  of  $123 \pm 2.6 \mu\text{g/mL}$  and a SI of 1.44. It was mentioned before that the higher molecular weight of sulfated polysaccharides, with higher fucose content and highly branched structures, contribute towards their antiviral activity. Fucoidan ( $3.90\text{--}500 \mu\text{g/mL}$ ) can prevent SARS-CoV-2 entry into the cell via binding to the glycoprotein [69]. According to the cytopathic effect inhibition assay, the loss of infectivity of HSV-1 and HAV viruses could be attributed to the effect of the sulfated polysaccharide SPF2 on the viral genome or the effect on the viral capsid protein. Queiroz et al. have investigated the role of fucoidan's sulfate and carboxyl groups in HIV inhibition. Even at modest concentrations, they found that fucoidan has a significant effect on reverse transcriptase in vitro. [70]. A few species of *Sargassum* were tested against HSV-1. Fucoidan was isolated from *S. polycystum*, and *S. ilicifolium* displayed strong activity with  $IC_{50}$  of 31.63 and 17.29  $\mu\text{g/mL}$ , respectively [71]. Water-soluble polysaccharides isolated from *Sargassum fluitans* also showed activity against HSV-1 with  $EC_{50}$  of 42.8  $\mu\text{g/mL}$  [72]. Fucoidan isolated from *Sargassum henslowianum* showed higher activity by using plaque reduction assay against HSV with  $IC_{50}$  of 0.89 and 0.48  $\mu\text{g/mL}$  against HSV-1 and HSV-2, respectively [16]. On the other hand, sulfated polysaccharide isolated from *Sargassum muticum* displayed very low activity against HSV. It was reported that the low antiviral activity in *Sargassum muticum* may be related to the lower sulfate groups [73]. In this research, we have proven the antiviral activity of sulfated polysaccharide from *S. asperifolium*, as a new species, against HSV-1 and HAV, which suggests a potential added-value product for seaweed stranding.

## 4. Conclusions

In the current study, sulfated polysaccharides (SPF1 and SPF2) were extracted from brown alga, *Sargassum asperifolium* harvested for the first time from Farasan Island, Jazan,

Saudi Arabia. The fucose-rich fraction (SPF2) was fully characterized by using FT-IR,  $^1\text{H}$ , and  $^{13}\text{C}$  NMR analysis. The findings of the in vitro antioxidant as well as antiviral activity against both HAV and HSV-1 viruses showed the potential broad activities of SPF2. Its biological activities are possibly attributed to its galactofucan skeleton compared to other classes of fucoidans. These comparative data suggested that the investigated polysaccharide (SPF2) could be a new additional candidate, as isolated from new species, a therapeutic agent against viruses. Focusing on new species in this field from a unique location, Farasan Island, can make a contribution to the field. These results need further investigation on the specific mechanism of viral inhibition.

**Author Contributions:** Conceptualization, A.A.A. and S.F.M.; methodology, A.A.A. and S.F.M.; investigation, A.A.A. and S.F.M.; writing—original draft preparation, S.F.M.; writing—review and editing, A.A.A.; supervision, A.A.A.; project administration, A.A.A.; funding acquisition, A.A.A. All authors have read and agreed to the published version of the manuscript.

**Funding:** Deanship of Scientific Research, Jazan University funded this research work through the Research Units Support Program, Support Number: RUP2-02.

**Data Availability Statement:** All the obtained data are presented in the manuscript.

**Acknowledgments:** The authors extend their appreciation to Deanship of Scientific Research, Jazan University, for supporting this research work through the Research Units Support Program, Support Number: RUP2-02.

**Conflicts of Interest:** The authors declare no conflict of interest.

## References

1. Wang, Y.; Di, Y.; Ye, J.; Wei, W. Study on the public psychological states and its related factors during the outbreak of coronavirus disease 2019 (COVID-19) in some regions of China. *Psychol. Health Med.* **2021**, *26*, 13–22. [[CrossRef](#)] [[PubMed](#)]
2. Hans, N.; Naik, S.N.; Malik, A. Platform Molecules from Algae by Using Supercritical  $\text{CO}_2$  and Subcritical Water Extraction. In *Handbook of Algal Technologies and Phytochemicals: Volume I: Food, Health and Nutraceutical Applications*; Ravishankar, G., Ambati, R.R., Eds.; CRC Press: Boca Raton, FL, USA, 2019; pp. 229–243.
3. Khalid, S.; Abbas, M.; Saeed, F.; Bader-Ul-Ain, H.; Ansar Rasul Suleria, H. Therapeutic potential of seaweed bioactive compounds. In *Seaweed Biomaterials*; Maiti, S., Ed.; IntechOpen: Rijeka, Croatia, 2018; pp. 7–25.
4. Mayer, A.M.S.; Rodríguez, A.D.; Berlinck, R.G.S.; Hamann, M.T. Marine pharmacology in 2005-6: Marine compounds with anthelmintic, antibacterial, anticoagulant, antifungal, anti-inflammatory, antimalarial, antiprotozoal, antituberculosis, and antiviral activities; affecting the cardiovascular, immune and nervous systems, and other miscellaneous mechanisms of action. *Biochim. Biophys. Acta* **2009**, *1790*, 283–308. [[PubMed](#)]
5. Deniaud-Bouët, E.; Hardouin, K.; Potin, P.; Kloareg, B.; Hervé, C. A review about brown algal cell walls and fucose-containing sulfated polysaccharides: Cell wall context, biomedical properties and key research challenges. *Carbohydr. Polym.* **2017**, *175*, 395–408. [[CrossRef](#)] [[PubMed](#)]
6. Muthukumar, J.; Chidambaram, R.; Sukumaran, S. Sulfated polysaccharides and its commercial applications in food industries—A review. *J. Food Sci. Technol.* **2021**, *58*, 2453–2466. [[CrossRef](#)] [[PubMed](#)]
7. Pereira, L. Seaweeds as source of bioactive substances and skin care therapy—Cosmeceuticals, algotherapy, and thalassotherapy. *Cosmetics* **2018**, *5*, 68. [[CrossRef](#)]
8. Kim, K.J.; Lee, O.H.; Lee, B.Y. Fucoidan, a sulfated polysaccharide, inhibits adipogenesis through the mitogen-activated protein kinase pathway in 3T3-L1 preadipocytes. *Life Sci.* **2010**, *86*, 791–797. [[CrossRef](#)] [[PubMed](#)]
9. Andri Frediansyah, S.S. The antiviral activity of iota-, kappa-, and lambda-carrageenan against COVID-19: A critical review. *Clin. Epidemiol. Glob. Health* **2021**, *12*, 100826. [[CrossRef](#)]
10. Jabeen, M.; Dutot, M.; Fagon, R.; Verrier, B.; Monge, C. Seaweed sulfated polysaccharides against respiratory viral infections. *Pharmaceutics* **2021**, *13*, 733. [[CrossRef](#)]
11. Reynolds, D.; Huesemann, M.; Edmundson, S.; Sims, A.; Hurst, B.; Cady, S.; Beirne, N.; Freeman, J.; Berger, A.; Gao, S. Viral inhibitors derived from macroalgae, microalgae, and cyanobacteria: A review of antiviral potential throughout pathogenesis. *Algal Res.* **2021**, *57*, 102331. [[CrossRef](#)]
12. Hu, T.; Liu, D.; Chen, Y.; Wu, J.; Wang, S. Antioxidant activity of sulfated polysaccharide fractions extracted from *Undaria pinnatifida* in vitro. *Int. J. Biol. Macromol.* **2020**, *46*, 193–198. [[CrossRef](#)]
13. Lim, S.J.; Mustapha, W.A.W.; Maskat, M.Y.; Latip, J.; Badri, K.H.; Hassan, O. Chemical properties and toxicology studies of fucoidan extracted from Malaysian *Sargassum binderi*. *Food Sci. Biotechnol.* **2016**, *25*, 23–29. [[CrossRef](#)]
14. Heald-Sargent, T.; Gallagher, T. Ready, set, fuse! The coronavirus spike protein and acquisition of fusion competence. *Viruses* **2012**, *4*, 557–580. [[CrossRef](#)] [[PubMed](#)]

15. Belouzard, S.; Millet, J.K.; Licitra, B.N.; Whittaker, G.R. Mechanisms of coronavirus cell entry mediated by the viral spike protein. *Viruses* **2012**, *4*, 1011–1033. [[CrossRef](#)] [[PubMed](#)]
16. Sun, Q.-L.; Li, Y.; Ni, L.-Q.; Li, Y.-X.; Cui, Y.-S.; Jiang, S.-L.; Xie, E.-Y.; Du, J.; Deng, F.; Dong, C.-X. Structural characterization and antiviral activity of two fucoidans from the brown algae *Sargassum henslowianum*. *Carbohydr. Polym.* **2020**, *229*, 115487. [[CrossRef](#)] [[PubMed](#)]
17. Laine, R.F.; Albecka, A.; van de Linde, S.; Rees, E.J.; Crump, C.M.; Kaminski, C.F. Structural analysis of herpes simplex virus by optical super-resolution imaging. *Nat. Commun.* **2015**, *6*, 5980–5990. [[CrossRef](#)] [[PubMed](#)]
18. Li, W.; Wang, X.-H.; Luo, Z.; Liu, L.-F.; Yan, C.; Yan, C.-Y.; Chen, G.-D.; Gao, H.; Duan, W.-J.; Kurihara, H.; et al. Traditional chinese medicine as a potential source for HSV-1 therapy by acting on virus or the susceptibility of host. *Int. J. Mol. Sci.* **2018**, *19*, 3266–3289. [[CrossRef](#)] [[PubMed](#)]
19. Richards, C.M.; Case, R.; Hirst, T.R.; Hill, T.J.; Williams, N.A. Protection against recurrent ocular herpes simplex virus type 1 disease after therapeutic vaccination of latently infected mice. *J. Virol.* **2003**, *77*, 6692–6699. [[CrossRef](#)] [[PubMed](#)]
20. Harris, S.A.; Harris, E.A. Herpes simplex virus type 1 and other pathogens are key causative factors in sporadic alzheimer's disease. *J. Alzheimers Dis.* **2015**, *48*, 319–353. [[CrossRef](#)]
21. Cristina, J.; Costa-Mattioli, M. Genetic variability and molecular evolution of hepatitis A virus. *Virus Res.* **2007**, *127*, 151–157. [[CrossRef](#)]
22. Mohamed, S.F.; Agili, F.A. Antiviral sulphated polysaccharide from brown algae *Padina pavonia* characterization and structure elucidation. *Int. J. ChemTech Res.* **2013**, *5*, 1469–1476.
23. Asker, M.S.; Mohamed, S.F.; El-Sayed, O.H. Chemical structure and antiviral activity of water-soluble sulfated polysaccharides from *Sargassum latifolium*. *J. Appl. Sci. Res.* **2007**, *3*, 1178–1185.
24. Josephine, A.; Nithya, K.; Amudha, G.; Veena, C.K.; Preetha, S.P.; Varalakshmi, P. Role of sulphated polysaccharides from *Sargassum wightii* in cyclosporine A-induced oxidative liver injury in rats. *BMC Pharmacol.* **2008**, *8*, 4–12. [[CrossRef](#)]
25. Mattio, L.; Payri, C.E. 190 years of *Sargassum* taxonomy, facing the advent of DNA phylogenies. *Bot. Rev.* **2011**, *77*, 31–70. [[CrossRef](#)]
26. Available online: <https://www.google.com/maps/place/Farasan+Island/@17.1544381,33.3202851,5z/data=!4m6!3m5!1s0x160853c66cd55563:0xb3938bc011e607f3!8m2!3d16.705833!4d41.983333!16zL20vMGJibjQ3?entry=tts> (accessed on 23 June 2023).
27. Silva, T.M.A.; Alves, L.G.; de Queiroz, K.C.S.; Santos, M.G.L.; Marques, C.T.; Chavante, S.F.; Rocha, H.A.O.; Leite, E.L. Partial characterization and anticoagulant activity of a heterofucan from the brown seaweed *Padina gymnospora*. *Braz. J. Med. Biol. Res.* **2005**, *38*, 523–533. [[CrossRef](#)] [[PubMed](#)]
28. Wang, C.-Y.; Chen, Y.-C. Extraction and characterization of fucoidan from six brown macroalgae. *J. Mar. Sci. Technol.* **2016**, *24*, 319–328.
29. Trabelsi, I.; Slima, S.B.; Ktari, N.; Bardaa, S.; Elkaroui, K.; Abdeslam, A.; Ben Salah, R. Purification, composition and biological activities of a novel heteropolysaccharide extracted from *Linum usitatissimum* L. seeds on laser burn wound. *Int. J. Biol. Macromol.* **2020**, *144*, 781–790. [[CrossRef](#)] [[PubMed](#)]
30. Sudhamani, S.R.; Tharanathan, R.N.; Prasad, M.S. Isolation and characterization of an extracellular polysaccharide from *Pseudomonas caryophylli* CFR 1705. *Carbohydr. Polym.* **2004**, *56*, 423–427. [[CrossRef](#)]
31. El-Newary, S.A.; Ibrahim, A.Y.; Asker, M.S.; Mahmoud, M.G.; El Awady, M.E. Production, characterization and biological activities of acidic exopolysaccharide from marine *Bacillus amyloliquefaciens* 3MS 2017. *Asian Pac. J. Trop. Med.* **2017**, *10*, 652–662. [[CrossRef](#)]
32. Kolmert, Å.; Wikström, P.; Hallberg, K.B. A fast and simple turbidimetric method for the determination of sulfate in sulfate-reducing bacterial cultures. *J. Microbiol. Methods* **2000**, *41*, 179–184. [[CrossRef](#)]
33. Jun, H.-L.; Lee, C.-H.; Song, G.-S.; Kim, Y.-S. Characterization of the pectic polysaccharides from pumpkin peel. *LWT J. Food Sci. Technol.* **2006**, *39*, 554–561. [[CrossRef](#)]
34. Wang, H.; Ooi, E.V.; Ang, P.O. Antiviral polysaccharides isolated from Hong Kong brown seaweed *Hydroclathrus clathratus*. *Sci Chin. C Life Sci.* **2007**, *50*, 611–618. [[CrossRef](#)] [[PubMed](#)]
35. You, L.; Gao, Q.; Feng, M.; Yang, B.; Ren, J.; Gu, L.; Cui, C.; Zhao, M. Structural characterisation of polysaccharides from *Tricholoma matsutake* and their antioxidant and antitumour activities. *Food Chem.* **2013**, *138*, 2242–2249. [[CrossRef](#)] [[PubMed](#)]
36. Bulu, M.; Dhruvo, J.S.; Beduin, M.; Amit, K.N. Extraction, characterization, haematocompatibility and antioxidant activity of linseed polysaccharide. *Carbohydr. Polym. Technol. Appl.* **2023**, *5*, 100321–100330.
37. Venkatesan, M.; Arumugam, V.; Pugalendi, R.; Ramachandran, K.; Sengodan, K.; Vijayan, S.R.; Sundaresan, U.; Ramachandran, S.; Pugazhendhi, A. Antioxidant, anticoagulant and mosquitocidal properties of water-soluble polysaccharides (WSPs) from Indian seaweeds. *Process Biochem.* **2019**, *84*, 196–204. [[CrossRef](#)]
38. Al-Salahi, R.; Alswaidan, I.; Marzouk, M. Cytotoxicity evaluation of a new set of 2-aminobenzo[de]iso-quinoline-1,3-diones. *Int. J. Mol. Sci.* **2014**, *15*, 22483–22491. [[CrossRef](#)] [[PubMed](#)]
39. Randazzo, W.; Piqueras, J.; Rodríguez-Díaz, J.; Aznar, R.; Sánchez, G. Improving efficiency of viability-qPCR for selective detection of infectious HAV in food and water samples. *J. Appl. Microbiol.* **2018**, *124*, 958–964. [[CrossRef](#)]
40. Pintó, R.M.; Diez, J.M.; Bosch, A. Use of the colonic carcinoma cell line CaCo-2 for in vivo amplification and detection of enteric viruses. *J. Med. Virol.* **1994**, *44*, 310–315. [[CrossRef](#)]

41. Vijayan, P.; Raghu, C.; Ashok, G.; Dhanaraj, S.A.; Suresh, B. Antiviral activity of medicinal plants of Nilgiris. *Ind. J. Med. Res.* **2004**, *120*, 24–29.
42. Mosmann, T. Rapid colorimetric assay for cellular growth and survival: Application to proliferation and cytotoxicity assays. *J. Immunol. Methods* **1983**, *65*, 55–63. [[CrossRef](#)]
43. Shehabeldine, A.M.; Elbahnasawy, M.A.; Hasaballah, A.I. Green phytosynthesis of silver nanoparticles using *Echinochloa stagnina* extract with reference to their antibacterial, cytotoxic, and larvicidal activities. *Bionanoscience* **2021**, *11*, 526–538. [[CrossRef](#)]
44. Al-Salahi, R.; Alswaidan, I.; Ghabbour, H.A.; Ezzeldin, E.; Elaasser, M.; Marzouk, M. Docking and antiherpetic activity of 2-aminobenzo[de]-isoquinoline-1,3-diones. *Molecules* **2015**, *20*, 5099–5111. [[CrossRef](#)] [[PubMed](#)]
45. Hu, J.M.; Hsiung, G.D. Evaluation of new antiviral agents: I. In vitro perspectives. *Antivir. Res.* **1989**, *11*, 217–232. [[CrossRef](#)] [[PubMed](#)]
46. Keivan, Z.; Moloud, A.Z.; Kohzad, S.; Zahra, R. Antiviral activity of Aloe vera against herpes simplex virus type 2: An in vitro study. *Afr. J. Adv. Biotechnol.* **2007**, *6*, 1770–1773. [[CrossRef](#)]
47. Ale, M.T.; Maruyama, H.; Tamauchi, H.; Mikkelsen, J.D.; Meyer, A.S. Fucoidan from *Sargassum* sp. and *Fucus vesiculosus* reduces cell viability of lung carcinoma and melanoma cells in vitro and activates natural killer cells in mice in vivo. *Int. J. Biol. Macromol.* **2011**, *49*, 331–336. [[CrossRef](#)] [[PubMed](#)]
48. Fletcher, H.R.; Biller, P.; Ross, A.B.; Adams, J.M.M. The seasonal variation of fucoidan within three species of brown macroalgae. *Algal Res.* **2017**, *22*, 79–86. [[CrossRef](#)]
49. Rioux, L.E.; Turgeon, S.L.; Beaulieu, M. Characterization of polysaccharides extracted from brown seaweeds. *Carbohydr. Polym.* **2007**, *69*, 530–537. [[CrossRef](#)]
50. Wang, C.-Y.; Wu, T.-C.; Hsieh, S.-L.; Tsai, Y.-H.; Yeh, C.-W.; Huang, C.-Y. Antioxidant activity and growth inhibition of human colon cancer cells by crude and purified fucoidan preparations extracted from *Sargassum cristaeifolium*. *J. Food Drug Anal.* **2015**, *23*, 766–777. [[CrossRef](#)]
51. Béress, A.; Wassermann, O.; Tahhan, S.; Bruhn, T.; Béress, L.; Kraiselburd, E.N.; Gonzalez, L.V.; de Motta, G.E.; Chavez, P.I. A new procedure for the isolation of anti-HIV compounds (polysaccharides and polyphenols) from the marine alga *Fucus vesiculosus*. *J. Nat. Prod.* **1993**, *56*, 478–488. [[CrossRef](#)]
52. Lee, S.-H.; Ko, C.-I.; Ahn, G.; You, S.; Kim, J.-S.; Heu, M.S.; Kim, J.; Jee, Y.; Jeon, Y.-J. Molecular characteristics and anti-inflammatory activity of the fucoidan extracted from *Ecklonia Cava*. *Carbohydr. Polym.* **2012**, *89*, 599–606. [[CrossRef](#)]
53. Li, B.; Lu, F.; Wei, X.; Zhao, R. Fucoidan: Structure and bioactivity. *Molecules* **2008**, *13*, 1671–1695. [[CrossRef](#)]
54. Synytsya, A.; Kim, W.-J.; Kim, S.-M.; Pohl, R.; Synytsya, A.; Kvasnička, F.; Čopíková, J.; Il Park, Y. Structure and antitumour activity of fucoidan isolated from sporophyll of Korean brown seaweed *Undaria pinnatifida*. *Carbohydr. Polym.* **2010**, *81*, 41–48. [[CrossRef](#)]
55. Zhang, Y.; Zeng, Y.; Men, Y.; Zhang, J.; Liu, H.; Sun, Y. Structural characterization and immunomodulatory activity of exopolysaccharides from submerged culture of *Auricularia auricula-judae*. *Int. J. Biol. Macromol.* **2018**, *115*, 978–984. [[CrossRef](#)] [[PubMed](#)]
56. Wei, C.; Zhang, Y.; Zhang, H.; Li, J.; Tao, W.; Linhardt, R.J.; Chen, S.; Ye, X. Physicochemical properties and conformations of water-soluble peach gums via different preparation methods. *Food Hydrocoll.* **2018**, *95*, 571–579. [[CrossRef](#)]
57. Ke, H.; Bao, T.; Chen, W. Polysaccharide from *Rubus chingii* Hu affords protection against palmitic acid-induced lipotoxicity in human hepatocytes. *Int. J. Biol. Macromol.* **2019**, *133*, 1063–1071. [[CrossRef](#)] [[PubMed](#)]
58. Wang, K.; Li, W.; Rui, X.; Chen, X.; Jiang, M.; Dong, M. Structural characterization and bioactivity of released exopolysaccharides from *Lactobacillus plantarum* 70810. *Int. J. Biol. Macromol.* **2014**, *67*, 71–78. [[CrossRef](#)] [[PubMed](#)]
59. Patankar, M.S.; Oehninger, S.; Barnett, T.; Williams, R.L.; Clark, G.F. A revised structure for fucoidan may explain some of its biological activities. *J. Biol. Chem.* **1993**, *268*, 21770–21776. [[CrossRef](#)]
60. Feng, F.; Zhou, Q.; Yang, Y.; Zhao, F.; Du, R.; Han, Y.; Xiao, H.; Zhou, Z. Characterization of highly branched dextran produced by *Leuconostoc citreum* B-2 from pineapple fermented product. *Int. J. Biol. Macromol.* **2018**, *113*, 45–50. [[CrossRef](#)]
61. Rani, R.P.; Anandharaj, M.; Sabhpathy, P.; Ravindran, A.D. Physicochemical and biological characterization of novel exopolysaccharide produced by *Bacillus tequilensis* FR9 isolated from chicken. *Int. J. Biol. Macromol.* **2017**, *96*, 1–10. [[CrossRef](#)]
62. Das, D.; Goyal, A. Characterization and biocompatibility of glucan: A safe food additive from probiotic *Lactobacillus plantarum* DM5. *J. Sci. Food Agric.* **2014**, *94*, 683–690. [[CrossRef](#)]
63. Bilan, M.I.; Grachev, A.A.; Ustuzhanina, N.E.; Shashkov, A.S.; Nifantiev, N.E.; Usov, A.I. A highly regular fraction of a fucoidan from the brown seaweed *Fucus distichus*. *Carbohydr. Res.* **2004**, *339*, 511–517. [[CrossRef](#)]
64. Hu, X.; Pang, X.; Wang, P.G.; Chen, M. Isolation and characterization of an antioxidant exopolysaccharide produced by *Bacillus* sp. S-1 from Sichuan Pickles. *Carbohydr. Polym.* **2019**, *204*, 9–16. [[CrossRef](#)]
65. Mulloy, B.; Mourão, P.A.S.; Gray, E. Structure/function studies of anticoagulant sulphated polysaccharides using NMR. *J. Biotechnol.* **2000**, *77*, 123–135. [[CrossRef](#)] [[PubMed](#)]
66. Ismail, M.M.; Amer, M.S. Characterization and biological properties of sulfated polysaccharides of *Corallina officinalis* and *Pterocladia capillacea*. *Acta Bot. Bras.* **2020**, *34*, 623–632. [[CrossRef](#)]
67. Zhong, R.; Chen, Y.; Ling, J.; Xia, Z.; Zhan, Y.; Sun, E.; Shi, Z.; Feng, L.; Jia, X.; Song, J.; et al. The toxicity and metabolism properties of herba epimedii flavonoids on larval and adult zebrafish. *Evid. Based Complement. Altern. Med.* **2019**, *2019*, 3745051–3745060.

68. Sae-Lao, T.; Tohtong, R.; Bates, D.O.; Wongprasert, K. Sulfated galactans from red seaweed *Gracilaria fisheri* target EGFR and inhibit cholangiocarcinoma cell proliferation. *Am. J. Chin. Med.* **2017**, *45*, 615–633. [[CrossRef](#)]
69. Song, S.; Peng, H.; Wang, Q.; Liu, Z.; Dong, X.; Wen, C.; Ai, C.; Zhang, Y.; Wang, Z.; Zhu, B. Inhibitory activities of marine sulfated polysaccharides against SARS-CoV-2. *Food Funct.* **2020**, *11*, 7415–7420. [[CrossRef](#)] [[PubMed](#)]
70. Queiroz, K.C.S.; Medeiros, V.P.; Queiroz, L.S.; Abreu, L.R.D.; Rocha, H.A.O.; Ferreira, C.V.; Jucá, M.B.; Aoyama, H.; Leite, E.L. Inhibition of reverse transcriptase activity of HIV by polysaccharides of brown algae. *Biomed. Pharmacother.* **2008**, *62*, 303–307. [[CrossRef](#)]
71. Dwi, L.W.; Ningsih, A.T.; Ita, W.; Rexie, M.; Anicia, H.; Christel, M.; Nathalie, B. The potential of cytotoxin and antiviral in *Sargassum polycystum* and *Sargassum ilicifolium*'s polysaccharides extract. *Indones. J. Mar. Sci.* **2020**, *25*, 91–96.
72. Gilles, B.; Edgar, C.; Romain, B.; Christel, M.; Nathalie, B.; Yolanda, F.; Daniel, R. Antiviral and cytotoxic activities of polysaccharides extracted from four tropical seaweed species. *Nat. Prod. Commun.* **2017**, *12*, 807–811.
73. Hugo, P.; Kévin, H.; Gilles, B.; Christel, M.; Stéphane, C.; Yolanda, F.; Daniel, R.; Nathalie, B. Sulfated polysaccharides from seaweed strandings as renewable source for potential antivirals against *Herpes simplex virus 1*. *Mar. Drugs* **2022**, *20*, 116–138.

**Disclaimer/Publisher's Note:** The statements, opinions and data contained in all publications are solely those of the individual author(s) and contributor(s) and not of MDPI and/or the editor(s). MDPI and/or the editor(s) disclaim responsibility for any injury to people or property resulting from any ideas, methods, instructions or products referred to in the content.